DC and AC Conductivity of Carbon Nanotubes−Polyepoxy Composites

Sophie Barrau,[†] Philippe Demont,*[,†] Alain Peigney,[‡] Christophe Laurent,[‡] and Colette Lacabanne[†]

Laboratoire de Physique des Polymères and Laboratoire de Chimie des Matériaux Inorganiques, CIRIMAT, UMR CNRS 5085, Université Paul Sabatier, 31062 Toulouse Cedex, France

Received August 5, 2002; Revised Manuscript Received March 26, 2003

ABSTRACT: The dc and ac conductivities of carbon nanotubes−polyepoxy composites have been investigated from 20 to 110 °C in the frequency range 10^{-2}−10^{6} Hz as a function of the conductive weight fraction p ranging from 0.04 to 2.5 wt %. The frequency dependence of the measured conductivity obeys the universal dynamic response (UDR): a dc plateau followed, above a critical frequency ω_c, by the ω^s power law with exponent $s \sim 0.6$−1. The dc conductivity follows a percolation scaling law: $\sigma_{dc} \propto (p - p_c)^t$ with $p_c = 0.3$ wt % and $t = 1.4$−1.8, according to the temperature. σ_{dc} reached 10^{-4} S/cm for 2.5 wt % CNTs content and increases with increasing temperature. Considering a biased random walk in three dimensions approach, we may explain the scaling law of ω_c with p and its proportionality to σ_{dc}. The universality of ac conduction in carbon nanotubes−polymer composites is examined by the construction of master curves.

Introduction

Polymers such as epoxy resin contain a very low concentration of free charge carriers and are therefore generally good electrical insulators. Epoxy resins were used as suitable matrices in several areas of industry, such as the aerospace industry in the fuselage and the facing layers of airliners and such as microelectronics in the insulators between adjacent planes of multilayers printed circuits board. But there are instances when an increased conductivity of the polymer is warranted, such as in applications that require electrostatic dissipation (antistatic materials) or electromagnetic radiation shielding.

The electrical conductivity of an insulating polymer can be altered by adding conducting particles like carbon black particles,[1−8] carbon fibers,[9] metallic fillers,[10,11] or intrinsically conducting polymers.[12−14] The conductivity of the composite material can thus be controlled by properly choosing the components, their shape, and their relative concentrations.

The use of carbon nanotubes (CNTs), discovered by Iijima in 1991,[15] in CNTs−polymer composites has attracted wide attention because of their extraordinary mechanical and electrical properties.[16−22] Compared to carbon fibers, CNTs have a larger aspect ratio, higher strength and flexibility, and lower density, making them ideal reinforcing fillers in nanocomposites.[23−29] Then conducting polymer structures may be developed at low loading of nanotube fillers due to the lower percolation thresholds needed for the high aspect ratio nanotube structures.[30−37] Carbon nanotubes can be either metallic or semiconducting, depending on their diameter and helicity.[17] Macroscopic single-wall carbon nanotube (SWCNT) samples, in the form of randomly oriented nanotube ropes, form a pseudo-metal with conductivity of approximately 10^3 S/cm .[21] In unaligned CNT pellets conductivities about 50 S/cm were obtained.[33,34,38] In mats of SWNTs the reported conductivity is on the order of 200 S/cm.[39]

Interaction between the CNTs and polymer matrix, the properties of the CNTs themselves (diameter, length, specific surface area, surface conductivity), and the dispersion of the CNTs within the polymer significantly affect the electrical conductivity of such composites. It is well-known that conductive fillers−insulating polymer composites becomes electrically conductive as the filler content exceeds a certain critical value attributed to a percolation phenomenon.[40] Below the percolation threshold, the conducting composite materials behave as insulators, where conductivity, increasing with temperature, is generally determined by thermally assisted hopping or charge tunneling between the conducting particles. The electrical percolation threshold is dependent on the matrix material or preparation process used. Sandler et al.[32] have developed composites on epoxy resins which exhibits a percolation threshold below 0.04 wt %. Very low percolation threshold was also obtained with multiwalled carbon nanotubes (MWNTs) dispersed in a conjugated polymer or in poly(vinyl alcohol).[36] Transport properties in SWNTs and MWNTs−PMMA composites have been reported by Benoit et al.[34] and Stephan et al.[37] where low percolation thresholds of 0.33 and 0.5 wt % were obtained at room temperature. MWNTs−polycarbonate composites display a higher percolation threshold between 1 and 2 wt %.[29] However, the composites with thermoplastic polymers have a higher conductivity compared to that of composites with thermoset polymer when CNTs contents above percolation threshold are investigated.

The present study focused on the conductivity behavior of an epoxy resin filled with conductive CNTs concentration in the vicinity of the insulator−conductor transition. We report our experimental results on the dependence of the conductivity on the frequency, temperature, and filler content. Percolation theory is used to analyze the experimental results.

[†] Laboratoire de Physique des Polymères.
[‡] Laboratoire de Chimie des Matériaux Inorganiques.
* Corresponding author: Fax 33-5-61556221, e-mail demont@cict.fr.

10.1021/ma021263b CCC: $25.00
Published on Web 06/14/2003

Experimental Section

Samples. A commercially available bisphenol A type epoxy resin (LY5641, Hexcel Composites) was used as a prepolymer with a viscosity of 1−1.4 Pa s and a density of 1.15 g cm^{-3} at 25 °C. As a curing agent, an amine hardener (HY2954, Hexcel Composites) was used according to the manufacturer's recommended resin/curing agent ratio 100/35.

Small amounts of carbon nanotubes (CNTs) were embedded in epoxy polymer matrix. CNTs were synthesized by a catalytic chemical vapor deposition (CCVD) method with a carbon content of 83 wt % (95 vol %).[41] Statistical studies on HRTEM images of individual CNTs have shown that more than 80% are single- or double-walled carbon nanotubes and almost 90% have diameters equal to or smaller than 3 nm.[42] Amorphous carbon is not observed. After extraction, CNTs were washed many times with distilled water and then with ethanol. CNTs were kept in ethanol prior to the dispersion in epoxy resin to avoid the packing of nanotubes. CNTs−polyepoxy composites were prepared by dispersion of weight amount of CNTs, ranging from 0.04 to 2.5%, in the epoxy matrix. Epoxy matrix density is about 1.2 g cm^{-3} while the density of CNTs can be accurately estimated at 1.8 g cm^{-3}. Therefore, we can estimate reasonably that the CNTs volume fraction represents the two-thirds of the weight fraction.

For each weight fraction, CNTs were first dispersed in ethanol in an ultrasonic bath at the room temperature for 2 h. The liquid epoxy resin was added to the dilute suspension of nanotubes, and the mixture was again sonicated for 1 h. This mixture was left in a vacuum oven at 80 °C for 1 h in order to completely evaporate the solvent. The mixture was stirred at 2000 rpm for 1 h. The hardener was then added and mixed mechanically at 2000 rpm for 15 min. The last mixture was poured into suitable molds and then returned to vacuum for 20 min for degassing. The curing of epoxy matrix was carried in the oven at 120 °C for 20 min and then at 145 °C for 4 h. Samples of 10 mm in diameter and 1 mm thick were obtained. All samples were carefully polished to control their flatness.

The quality of the carbon nanotubes dispersion was examined by scanning electron microscopy (SEM). Samples were fractured in liquid nitrogen, and fracture surfaces of composites were observed. SEM micrographs reveal the presence of bundles of nanotubes fairly well randomly dispersed throughout the epoxy matrix. The bundle diameters are in the range 40−70 nm.

AC Conductivity. The ac conductivity measurements were performed in the frequency range between 10^{-2} and 10^{6} Hz using a Solartron-Schlumberger gain/phase analyzer SI 1260 together with a Novocontrol interface (broad-band dielectric converter). The ac output voltage was adjusted to 0.5 V. The measurements covered a temperature range from 20 to 110 °C using a nitrogen gas-controlled heating system (Quatro Novocontrol). The frequency sweeps were carried out when sample temperature was stable within ±0.2 °C. Nanocomposite samples were placed between two gold-plated brass electrodes that were pressed together with a micrometer screw. The dc conductivity σ_{dc} of the composites was determined from the frequency dependency of the ac conductivity $\sigma_{ac}(\omega)$ as the value of the conductivity in the region of the low-frequency plateau.

Results and Discussion

DC Conductivity. Figure 1 shows the frequency dependence of the real part, $\sigma'(\omega)$, of the complex electrical conductivity, for various carbon nanotubes weight content p in polyepoxy, measured at room temperature (20 °C). The bulk conductivity of the pure epoxy increases with increasing frequency as expected for an insulator material with a value about 10^{-16} S/cm at 10^{-1} s^{-1}. From 0.3 wt % we observe that $\sigma'(\omega)$ becomes independent of frequency at the lower frequencies of measurement and is identified as the dc conductivity, σ_{dc}. No decrease of conductivity with decreasing frequency at very low frequencies is observed, so that the electrode polarization is negligible. Above a characteristic onset frequency ω_c, the conductivity increases with increasing frequency. The frequency region of constant conductivity extends to higher frequencies with increasing weight fraction of CNTs. The frequency dependence of the alternative current (ac) conductivity follows a power law behavior. $\sigma'(\omega)$ or the total ac conductivity can be then represented by the following equation

$$\sigma'(\omega) = \sigma(0) + \sigma_{ac}(\omega) = \sigma_{dc} + A\omega^{s} \qquad (1)$$

where ω is the angular frequency, σ_{dc} is the independent frequency conductivity or dc conductivity (at $\omega \rightarrow 0$), A is the constant dependent on temperature T, and s is an exponent dependent on both frequency and temperature with values in the range 0−1. This type of behavior was noted by Jonscher, who called it the "universal dynamic response" (UDR)[43,44] because of a wide variety of materials that displayed such behavior.

The value of σ_{dc} can be estimated from the plateau values of conductivity in the $\sigma'(\omega)-\omega$ plot. There exists for each composition a critical frequency ω_c beyond which a power law is followed. The experimental definition of the critical frequency ω_c proposed by Kilbride et al.,[36] i.e., ω_c such as $\sigma(\omega_c) = 1.1\sigma_{dc}$, is applied to the frequency-dependent conductivity curves reported in Figure 1. The parameters σ_{dc} and ω_c are reported in Table 1 for the different weight fractions of CNTs in epoxy. It is clear that σ_{dc} and ω_c increase with increasing weight fraction of CNTs at room temperature. The room

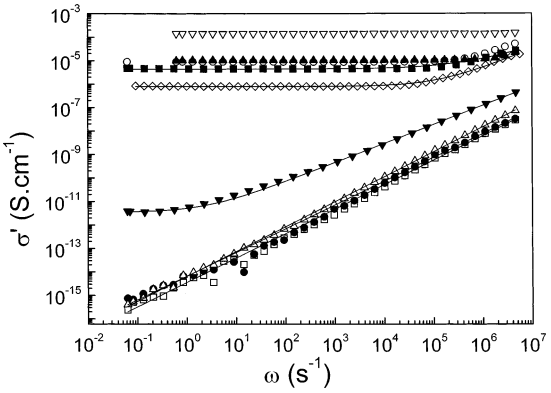

Figure 1. Frequency dependence of the real part σ' of the complex conductivity for different carbon nanotubes weight fraction p at 20 °C: (□) 0, (●) 0.04, (△) 0.2, (▼) 0.3, (◇) 0.4, (■) 0.6, (○) 0.8, (▲) 1.5, and (▽) 2.5 wt %. The solid lines are fits to eq 1.

Table 1. Parameters Describing Charge Transport Properties in CNTs−Polyepoxy Composites[a]

p (wt %)	σ_{dc} (S/cm)	ω_c (s^{-1})	s	A
0	2.4×10^{-16}		1.04 ± 0.01	3×10^{-15}
0.04	7.6×10^{-16}		1.01 ± 0.02	5×10^{-15}
0.2	4.0×10^{-16}		1.06 ± 0.01	6×10^{-15}
0.3	3.5×10^{-12}	0.28	0.81 ± 0.01	2×10^{-12}
0.4	7.9×10^{-7}	2.6×10^{4}	0.84 ± 0.02	4×10^{-11}
0.6	4.4×10^{-6}	1.0×10^{5}	0.65 ± 0.08	1×10^{-9}
0.8	8.7×10^{-6}	1.6×10^{5}		
1.5	9.9×10^{-6}	6.4×10^{5}		
2.5	1.3×10^{-4}	3.0×10^{6}		

[a] σ_{dc} stands for the room temperature dc conductivity, ω_c for the critical or crossover frequency, s and A for the parameters in eq 1.

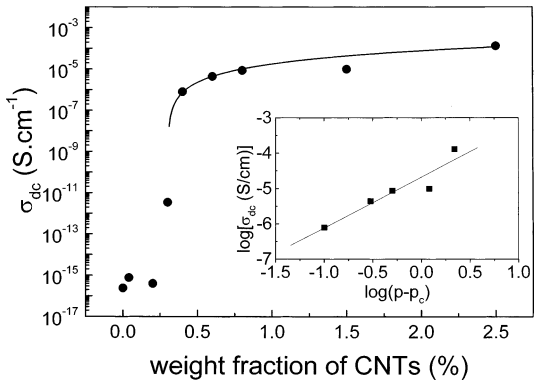

Figure 2. Dependence of the dc conductivity on the CNTs weight fraction p at 20 °C. The percolation threshold p_c is about 0.3 wt %. The solid line is a fit to the scaling law of the percolation theory (eq 2) using the parameters listed in Table 1. The inset shows the percolation scaling law between log σ and log($p - p_c$) where the solid line corresponds to the best fitted line.

dc conductivity of the CNTs−polyepoxy composite is shown in Figure 2 as a function of the weight fraction of CNTs. Between 0.2 and 0.4 wt %, the composite displays a dramatic increase by 10 orders of magnitude, and the conductivity levels off for higher concentrations, after a further addition of nanotubes. The conductivity of the 2.5 wt % sample was measured to be 1×10^{-4} S/cm, far below that of a SWNT rope material[21] or bundles of SWNTs.[35]

An abrupt percolation threshold p_c of the dc conductivity was observed at 0.3 wt % CNTs, indicating the existence of a percolating path via connecting CNTs. At this stage, the conductivity of the composite is controlled by the conducting CNTs. The dc conductivity is due to the formation of a network of CNTs within the epoxy matrix. The high aspect ratio and the dispersion of CNTs in the epoxy matrix allow achieving the percolation at very low weight fraction of nanotubes. Percolation theory defines an insulator−conductor transition and a corresponding threshold of the conductive filler concentration p_c, via the equation

$$\sigma = \sigma_0(p - p_c)^t \quad \text{for } p > p_c \tag{2}$$

where σ_0 is a constant, p the weight fraction of nanotubes, and t the critical exponent.[40] The data are fitted to the scaling law, and the best-fitted values are for $p_c = 0.3$ wt %, $\sigma_0 = 2 \times 10^{-5}$ S/cm, and $t = 1.44 \pm 0.30$. As mentioned previously, extrapolation to $p = 100\%$ using eq 2 gives a conductivity of 2×10^{-5} S/cm, which is 6 orders of magnitude lower than the conductivity measured in bundles of SWNTs.[34,38] This behavior is similar to that found in MWNTs−PmPV[36] or in MWNTs−PMMA[37] composite thin films. Kilbride et al.[36] have been attributed to a such discrepancy in the conductivity values to a coating of the individual nanotubes by a polymer insulating surface resulting in a poor electrical contact between nanotubes. If σ_{dc} is reduced to the volume fraction of nanotubes, we found a conductivity about 10^{-2} S/cm for the highest content, a value still much lower than the CNTs pellets conductivity, i.e., 50 S/cm.[33,34] Stephan et al.[37] suggest that large contact resistances could also induce a further limitation of the conductivity to explain their low value (10^{-5} S/cm) for 16 wt % of MWNTs in PMMA matrix.

The conductivity critical exponent's value is smaller than the universal value to three-dimensional percolating systems ($t = 1.94$).[40] The percolation phenomenon and more exactly the percolation threshold p_c are temperature-independent in the investigated temperature range. We find $t = 1.61 \pm 0.20$ and 1.71 ± 0.20 for $T = 50$ and 100 °C, respectively. The critical exponent increases with increasing temperature and tends toward the value predicted by 3D percolation theory of randomly distributed objects. A such low value of the exponent t is previously obtained in MWNTs−PmPV composite thin films,[36] i.e., $t = 1.36$. As reported by Kilbride et al.,[36] values of t around 1.3 have been observed in polyaniline−PMMA[45,46] or carbon black−polyethylene[47] composites. These values, lower than the universal value for three-dimensional percolating systems, can mean that the percolation takes place in a network displaying more "dead arms" than a classical random network. The increase of the critical exponent t value with increasing temperature could be then associated with the reduction in the number of "dead arms" present when the temperature approaches the glass transition temperature.

A general relationship between the percolation threshold of systems of various objets and their associated excluded volume has been discussed by Balberg et al.[48] In the isotropic case of randomly long sticks (length L and radius r) the proposed relation is

$$(L/r)f_c \approx 3 \tag{3}$$

where L/r and f_c are the aspect ratio and the critical volume fraction of the stick, respectively. Assuming the stick is a bundle of carbon nanotubes and using eq 3 and $f_c = 0.2$ vol %, we find $L/r = 1500$, which is agreement with a conduction through long sticks, i.e., the CNTs bundles.

This high aspect makes the percolation possible with a very small content of CNTs, i.e., 0.3 wt %. This low percolation threshold in carbon nanotubes−polymer composites changes with nanotube structure, as in nanotubes−PMMA composites where the use of SWNTs[34] results in lower threshold and higher conductivity values than MWNTs.[37] However, Sandler et al.[32] reported, for the same epoxy matrix and process used, but with MWNTs of typical diameter range from 5 to 10 nm and synthesized by CVD, a percolation threshold 10 times as small. Such a variation between percolation threshold values is surprising because more than 90% of our CNTs are SWNTs and DWNTs with smaller diameter than MWNTs. This observation confirms that the conduction in our composites is due mainly to the CNT bundles.

Above the percolation threshold a finite conductivity led to a plateau at low frequency corresponding to the electrical response of the percolating network. Investigations above the percolation threshold at various low ac voltages were performed to identify electric nonlinearity in CNTs composites. Figure 3 displays the dependence of the sample conductivity $\sigma'(\omega)$ on the ac applied voltage for 0.8 wt % of CNTs at 20 °C. It is clear from Figure 3 that only the dc contribution to σ' is affected by the voltage variation. In the frequency range where dc conductivity is observed ($\omega < 10^3$ s^{-1}), conductivity increases with increasing voltage. The inset in Figure 3 shows the current−voltage ($I-V$) characteristics (CVC) associated with the dc conductivity. At voltage smaller than 1 V, the CVC displays a linear

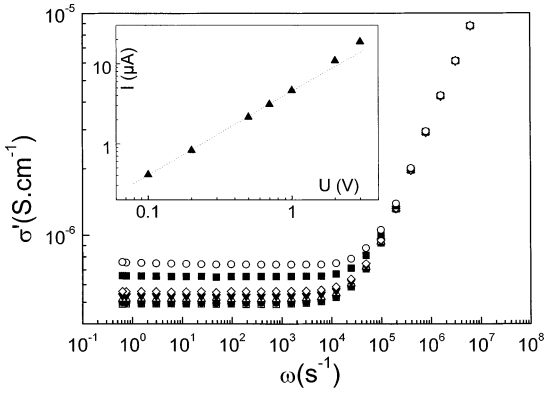

Figure 3. Room temperature frequency dependence of the real part σ' of the complex conductivity at various ac voltage for 0.8 wt % of CNTs: (□) 0.1, (●) 0.2, (△) 0.5, (▼) 0.7, (◇) 1, (■) 2, and (○) 3 V. The inset shows the logarithmic current−voltage characteristics (CVC).

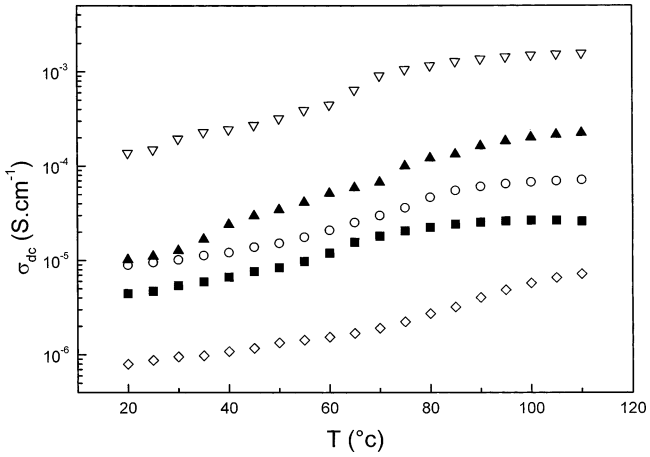

Figure 4. Temperature dependence of the dc conductivity above the percolation threshold p_c in the temperature range 20−110 °C: (◇) 0.4, (■) 0.6, (○) 0.8, (▲) 1.5, and (▽) 2.5 wt %.

pattern; i.e., the conduction is ohmic. Above 1 V, the current departs slightly from the voltage linear dependence. Nevertheless, significant nonohmic behavior exhibition requires higher voltage values. The observed ohmic behavior above the percolation threshold is in agreement with the $I-V$ characteristics reported by Kilbride et al. in MWNTs−PmPV composite thin films[36] or carried by Stephan et al. in MWNTs−PMMA composites.[37] Benoit[49] has shown that the shape of $I-V$ characteristics in SWNTS−MMA composites depends on the nanotubes content, temperature, and electrical field strength; i.e., nonlinearity increases with increasing electric field and decreasing temperature and nanotubes content. In Langmuir−Blodgett films containing SWNTs bundles, the room temperature $I-V$ characteristic shows a linear dependence.[50] Watts et al.[51] have found that the conducting nanotube−polystyrene composite is essentially an ohmic conductor at room temperature. Kim et al. have reported that the $I-V$ characteristics in mats of SWNTs are linear above 15 K, and nonohmic behavior occurs only at very low temperatures.[52] In consideration of these mentioned works and the experimental parameters used here, i.e., a low electric field (<30 V/cm), room temperature, and carbon nanotubes content $p > p_c$, the observed ohmic behavior was therefore expected. At sufficiently high concentrations of carbon nanotubes in the composite, such as 0.8 wt %, conduction is predominantly achieved through the nanotube bundle contacts, and the composite behaves as a conductor. If, as assumed by Stephan et al.,[37] nonlinear $I-V$ characteristics set in CNTs−polymer composites are due to the charge transfer process from one tube or bundle to another across the polymer, we can then exclude therefore a fully insulating polymer layer between carbon nanotubes bundles. Indeed, this ohmic behavior is not in agreement with the idea that nanotubes or bundles are separated by a thick polymer barrier as suggested by the low value of the critical exponent t and the relatively low value of the composites conductivity, even at high CNTs content, compared with the reported values in pure SWNTs or MWNTs.

Temperature Dependence of the DC Conductivity. To discuss what mechanism controls the conduction of CNTs−polyepoxy composites, the characterization of the temperature dependence behavior of the dc conductivity is required. The temperature dependence of the dc conductivity has been investigated for temperature between 20 and 110 °C for $p \geq p_c$. In Figure 4 the dc conductivity is plotted as a function of the temperature. The presented curves show that the dc conductivity varies poorly with the temperature above the percolation threshold; i.e., the variation is less than 2 decades. In the investigated range of temperature the dc conductivity increases with temperature characteristics of a nonmetallic behavior. A weak change of the curve slope is observed in the range 50−70 °C, a temperature range at which a secondary mechanical relaxation process occurs using mechanical spectrometry at a frequency of 1 Hz.[53] When the temperature approaches the glass transition region of the composite, σ_{dc} tends to be independent of the temperature for all the CNTs weight contents above the percolation threshold. Figure 4 shows too that the temperature dependence of dc conductivity does not depend on the CNTs content, and we can reasonably think that the conduction at room temperature is controlled here by the topology of the system, i.e., by the connectivity of the conductive network.

In carbon black composites, tunneling conduction has been reported to explain the conduction mechanism and the nature of the contacts between conductive clusters.[2,6,54] In these systems, electrical conductivity is ascribed to tunneling though a potential barrier of varying height due to thermal fluctuations. For a random distribution of the conducting particles, it can be shown that the mean average distance among particles is proportional to $p^{-1/3}$ and log σ_{dc} is proportional to $p^{-1/3}$, too. A linear relation between log σ_{dc} and $p^{-1/3}$ is an indication that tunneling conduction may be present in the samples.[2,6,36] In Figure 5, this relation is tested at three temperatures, and though the σ_{dc} value is too small for $p = 1.5$ wt %, the expected linear relation is accurately observed.

If some indications for tunneling effect in the charge carriers transport through the composites are present, the temperature dependence for the dc conductivity does not obey the model of the thermal fluctuation-induced tunneling (FIT) through thin barriers proposed by Sheng.[54,55] A theoretical expression for tunneling conductivity was obtained for disordered materials characterized by large conducting regions separated by potential barriers. The temperature dependence of the conductivity derives from thermally activated voltage

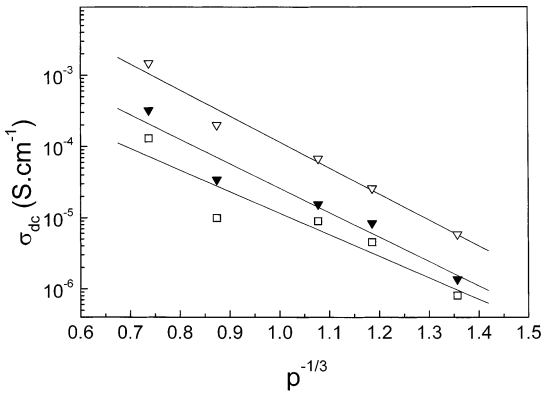

Figure 5. Plot of log σ_{dc} as the function of CNTs weight fraction $p^{-1/3}$ at different temperatures: (□) 20, (▼) 50, and (▽) 100 °C.

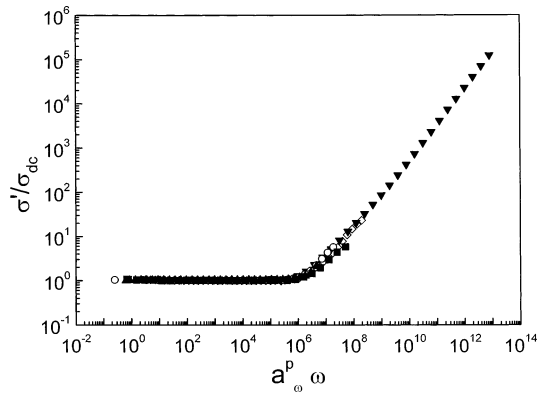

Figure 6. Master curve as a function of $[\sigma'(\omega,T)/\sigma_{dc}]$ as a function of $a^p_\omega\,\omega$ for $p \geq p_c$: (▼) 0.3, (◇) 0.4, (■) 0.6, (○) 0.8, (▲) 1.5, and (▽) 2.5 wt %.

fluctuations across insulating regions, which modulate the effective barrier. Sheng[55] found the following relationship for the conductivity:

$$\sigma_{dc}(T) = \sigma_0 \exp\left[-\frac{T_1}{T + T_0}\right] \tag{4}$$

where T_1 represents the energy required for an electron to cross the insulator gap between conductive particles aggregates and T_0 is the temperature above which the thermal activated conduction over the barrier begins to occur. No accurate fit to the conductivity data using eq 4 is obtained in the investigated temperature range. The simple thermal activation model describes the temperature dependence of the dc conductivity, and we cannot conclude that a mechanism of tunneling conduction is present in the CNTs−polymer composites. Localized molecular motions responsible of the sub-glass relaxation process of the polymer matrix in the range 50−70 °C[53] could alter the tunneling mechanism of the charge carriers between bundles of CNTs. Conductivity data at temperatures below 20 °C would confirm or contradict tunneling in theses composites.

AC Conductivity. Connor et al.[56] have reported in their investigations of conductor−polymer composites that the shapes of the conductivity curves were independent of conductor particles content p, and only the dc conductivity and critical frequency ω_c depend on p^2. They construct a p-independent master curve of the normalized conductivity, σ'/σ_{dc}, as a function of frequency and shift factor depending on p. In Figure 6, the scaled frequency of the real part of the complex conductivity for $p \geq p_c$ is shown. By plotting σ'/σ_{dc} vs $a^p_\omega\,\omega$, the conductivity data fall on one single curve where the shift factor a^p_ω is defined as

$$a^p_\omega = \frac{\omega_c^{p\ ref}}{\omega_c^p} \tag{5}$$

Here the reference content was $p_{ref} = 2.5$ wt % with $\omega_c^{p\ ref} = 3.0 \times 10^6$ s^{-1}.

As shown in Figure 1, the ω^s power law, characteristic of transport in disordered systems, is well present in the frequency response of the conductivity in CNTs−polyepoxy composites. To analyze the ac conductivity, the dc contribution σ_{dc} was subtracted from $\sigma'(\omega)$ data. Then the values of the exponent s for different weight fraction of CNTs at room temperature were determined from the linear slope of the $\log(\sigma' - \sigma_{dc})-\log\,\omega$ curve. The parameters A and s are reported in Table 1 for the different weight fractions of CNTs. Above 0.6 wt %, the frequency range where the power law is observed is too limited on the high-frequency side to determine accurately the s value. Because of the large frequency-independent contribution and the high crossover frequency, it is difficult to obtain the limiting slope at higher CNTs content.

Above the critical frequency and for $p > p_c$, the increase of conductivity with increasing conductivity, according a power law behavior, is similar to the one observed in MWNTs−PmPV composites thin films[36] where the exponent s is about 0.92. To compare CNTs embedded in a conjugated polymer or in epoxy resin through the frequency dependence of the ac conductivity, we continue the idea, unfolded by Kilbride et al.,[36] to explain the critical frequency behavior with the CNTs content. They suggest that charge carriers undergo a biased random walk along the conducting network with a relevant distance L that is traveled through the network and then consider that the frequency required by this carrier to travel L in one-half period is given by

$$\omega \propto L^{-1/a}; \quad 0.5 < a < 1 \tag{6}$$

where a describes the level of bias imposed on the walk by the application of an external field. They assume that $\omega_c \equiv \omega_\xi$, where ω_ξ is the frequency at which a carrier travels a distance equivalent to the correlation length ξ of the percolating system. Then ω_ξ is given by

$$\omega_\xi \propto \xi^{-1/a} \tag{7}$$

Since in any network the correlation length is expressed as

$$\xi \propto |p - p_c|^{-\nu} \tag{8}$$

the angular critical frequency can be then expressed as

$$\omega_c \propto (p - p_c)^{\nu/a} \tag{9}$$

where $\nu = 0.88$ for a lattice space dimension, $d = 3$. The critical angular frequency, measured on samples containing 0.4−2.5 wt % CNTs, is plotted as a function of $(p - p_c)$ on a log−log scale in Figure 7. From the slope of the straight line, ν/a is found to be equal to 1.48 ± 0.15 and then giving $a = 0.60$ (0.76 in MWNTs−PmPV composites) well within the criteria for a. According to

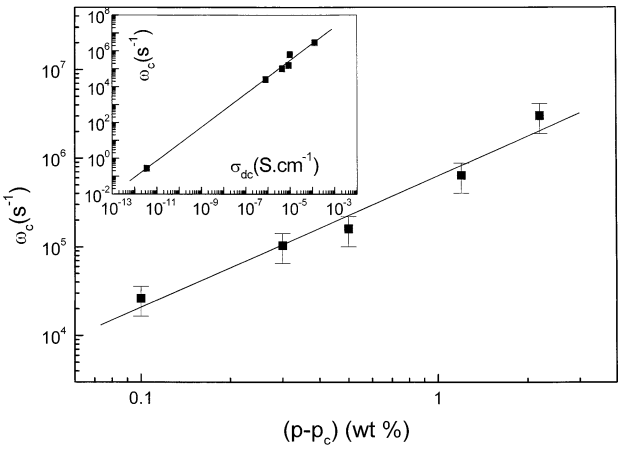

Figure 7. A log−log plot of critical frequency ω_c vs $p - p_c$. The solid line is a fit to power law using eq 9. The inset shows the correlation between ω_c and the dc conductivity σ_{dc} at room temperature . The solid line represents the best fitted line for various CNTs content above the percolation threshold. The error bars are within the thickness of the symbols.

Kilbride, this value suggests a weakly biased random walk through a three-dimensional structure. The critical frequency is found to be closely related to dc conductivity at room temperature and for various CNTs content as can be seen in the inset of Figure 7. The data are the best fitted by the power law

$$\omega_c(p) \propto \sigma_{dc}^{b}(p) \quad \text{for } p > p_c \tag{10}$$

where the exponent has the value $b = 0.93 \pm 0.03$. This behavior has been reported by Dyre and Schroder[44] as one of the ac characteristics of the vast majority of disordered solids.

Using eqs 9 and 10, the dc conductivity can be expressed by

$$\sigma \propto (p - p_c)^{\nu/ab} \quad \text{for } p > p_c \tag{11}$$

and according to eq 2, $t = \nu/ab = 1.48/0.93 = 1.59$. This value, close to the value obtained from the fit of the dc conductivity data to eq 2, supports that the use of a biased random walk approach and the assumption $\omega_c \equiv \omega_\xi$ are correct.

For CNTs content below the percolation threshold and above a temperature-dependent critical frequency, all the ac conductivity data obey the same power law ω^s with $s \sim 1$ characteristic of a typical dielectric behavior as expected in insulator materials. The inset in Figure 8 shows the dispersion of the real part of the complex conductivity as a function of frequency at various temperatures below the glass transition of epoxy for $p = 0.4$ wt %. All the frequency curves presented reveal similar features: a dc plateau up to certain critical frequency followed by a gradual but increase of the conductivity at higher frequencies. In Figure 8, the scaled frequency dependence of the real part of the conductivity for the CNTs composite with $p = 0.4$ wt % is shown. By plotting (σ'/σ_{dc}) vs $(\omega/\sigma_{dc}T)$, the conductivity data between 20 and 110 °C fall on one single curve. This frequency and temperature scaling is generally observed for the conduction in disordered materials.[44,57−59] The temperature dependence of the power law exponent s is shown in Figure 9 for $p = 0.4$ wt %. It is clear that the exponent decreases with increasing temperature. This behavior associated with the s increase with increasing frequency is consistent with the presence of a correlated barrier hopping (CBH) mechanism proposed by Pike[60] and Elliot,[61] where s is written as

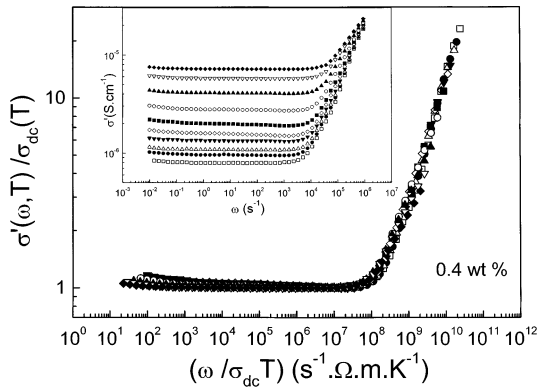

Figure 8. Scaled conductivity $[\sigma'(\omega,T)/\sigma_{dc}]$ vs scaled frequency $[\omega/(\sigma_{dc}T)]$ for $p = 0.4$ wt % of CNTs in the temperature range 20−110 °C: (□) 20, (●) 30, (△) 40, (▼) 50, (◇) 60, (■) 70, (○) 80, (▲) 90, (▽) 100, and (◆) 110 °C. The inset shows the frequency dependence of the real part σ' of the complex conductivity at temperature ranging from 20 to 120 °C for $p = 0.4$ wt %.

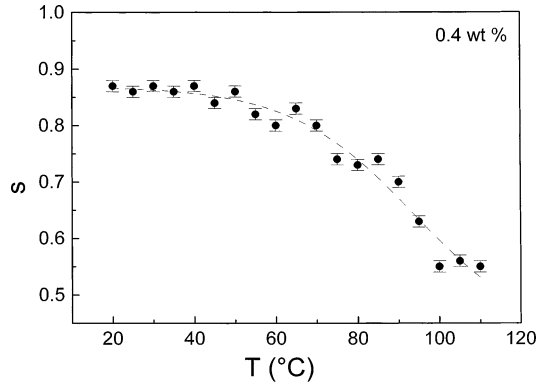

Figure 9. Temperature dependence of the conductivity exponent s for $p = 0.4$ wt % of CNTs.

$$s = 1 - \frac{6k_BT}{W_M - k_BT\ln(1/\omega\tau_0)} \tag{12}$$

where W_M is the maximum barrier height and τ_0 is a characteristic relaxation time which is on the order of an atom vibrational period $\tau_0 \sim 10^{-13}$ s. Also, eq 12 predicts that s decreases with increasing temperatures at large W_M/k_BT. But no accurate fit to the s temperature dependence is obtained. Nevertheless, the existence of two regimes in the temperature dependence behavior of the ac conductivity is also seen in the temperature variation of the exponent s. Below 50 °C the exponent is constant and is about 0.87, but above 50 °C the value of s drops rapidly. A similar change in the temperature behavior, although weak, has been previously pointed out for the dc conductivity in the temperature range 50−70 °C, as shown in Figure 4. Studies of the temperature dependence of the ac conductivity above the glass transition of the polymer matrix would clarify the accurate role of the polymer matrix in the transport properties of these composites.

Conclusions

The dc and ac electrical properties of composites, made by dispersing the high-conductivity carbon nano-

tubes in the insulating matrix of epoxy resin, have been investigated in the vitreous state. The experimental results showed a dc conductivity percolation at a low threshold $p_c = 0.3$ wt % with a critical exponent $t = 1.44$ at room temperature which increases as temperature approaches the glass transition temperature T_g. The behavior at low voltage and above the percolation threshold follows an ohmic-type law at room temperature. Indications that tunneling conduction may be the main conduction mechanism of the CNTs−epoxy composites are presented. The insulating polymer plays an important role in determining the transport mechanism of composites. These observations are in agreement with the experimental results reported in other carbon nanotube−polymer composites, suggesting that the nature of polymer host is not essential in the transport properties. Further temperature investigations below room temperature and above the glass transition temperature are necessary to predict the conduction mechanism in these nanocomposites.

The frequency dependence of the measured conductivity shows typical characteristics of the universal dynamic response (UDR). Above a CNTs content dependent critical angular frequency ω_c the conductivity follows a power law $A\omega^s$ with $0.5 < s \leq 1$ being characteristic for hopping conduction. The critical frequency ω_c follows the scaling law $\omega_c \propto (p - p_c)^{\nu/a}$ with $\nu/a = 1.48$ due to the variation of the correlation length with nanotube content as previously observed in MWNTs−PmPV composites. The ω_c behavior of the dispersion in ac conductivity is well represented by a model based on a weakly biased random walk in a three-dimensional network. The proportionality between ω_c and σ_{dc} strengthens the firmness of this approach. A master curve is obtained by introducing the critical angular frequency in a shift factor. The created master curve well describes the frequency behavior of the conductivity at all the compositions above p_c. When scaled to dc conductivity and at a given CNTs content p, the frequency-dependent conductivity shows a unique dependence on frequency, independent of the temperature. The exponent s is a function of the temperature and decreases as CNTs content increases above percolation threshold p_c in the vicinity of p_c. This exponent decreases with the increase of temperature as expected in the CBH model.

We have shown that the observations reported throughout the dc and ac investigations of carbon nanotubes−polyepoxy composites exceed the field of polyepoxy and may apply correctly to any carbon nanotubes−polymer composite.

References and Notes

(1) Tchmutin, I. A.; Ponomarenko, A. T.; Shevchenko, V. G.; Ryvkina, N. G.; Klason, C.; McQueen, D. H. *J. Polym. Sci.., Part B*: *Polym. Phys.* **1997**, *36*, 1847.
(2) Connor, M. T.; Roy, S.; Ezquerra, T. A.; Balta Calleja, F. J. *Phys. Rev. B* **1998**, *57*, 2286.
(3) Broom, H. B.; Reedijk, J. A.; Martens, H. C. F.; Adriaanse, L. J.; de Jongh, L. J.; Michels, M. A. J. *Phys. Status Solidi B* **1998**, *205*, 103.
(4) Foulger, S. H. *J. Appl. Polym. Sci.* **1999**, *72*, 1573.
(5) Flandin, F.; Prasse, T.; Schueler, R.; Schulte, K.; Bauhofer, W.; Cavaille, J.-Y. *Phy. Rev. B* **1999**, *59*, 14349.
(6) Alexander, M. G. *Mater. Res. Bull.* **1999**, *34*, 603.
(7) Zois, H.; Apekis, L.; Omastova, M. *Macromol. Symp.* **2001**, *170*, 249.
(8) Jäger, K. M.; McQueen, D. H. *Polymer* **2001**, *42*, 9575.
(9) Lozano, K.; Bonilla- Rios, J.; Barrera, V. *J. Appl. Polym. Sci.* **2001**, *80*, 1162.
(10) Parras, G. C.; Manolakaki, E.; Tsangaris, G. M. *Composites, Part A* **2002**, *33*, 375.
(11) Mamunya, Y.; Davydenko, V. V.; Pissis, P.; Lebedev, E. V. *Eur. Polym. J.* **2002**, *38*, 1887.
(12) Cassignol, C.; Cavarero, M.; Boudet, A.; Ricard, A. *Polymer* **1999**, *5*, 1139.
(13) Dutta, P.; Biswas, S.; Ghosh, M.; De, S. K.; Chatterjee, S. *Synth. Met.* **2001**, *122*, 455.
(14) Bhattacharyya, S.; Saha, S. K.; Mandal, T. K.; Mandal, B. M.; Chakravorty, D.; Goswami, K. *J. Appl. Phys.* **2001**, *89*, 5547.
(15) Iijima, S. *Nature (London)* **1991**, *354*, 56.
(16) Ajayan, P. M.; Stephan, O.; Colliex, C.; Trauth, D. *Science* **1994**, *265*, 1212.
(17) Saito, R.; Fujita, M.; Dresselhaus, G.; Dresselhaus, M. S. *Appl. Phys. Lett.* **1992**, *60*, 2204.
(18) Dresselhaus, M. S.; Dresselhaus, G.; Eklund, P. In *Science of Fullerenes and Carbon Nanotubes*; Academic Press: New York, 1996.
(19) Ebbesen, T. W. In *Carbon Nanotubes*: *Preparation and Properties*; CRC Press: Boca Raton, FL, 1997.
(20) Wildoer, J. W. G.; Venema, L. C.; Rinzler; A. G.; Smalley; R. E.; Dekker, C. *Nature (London)* **1998**, *391*, 59.
(21) Fischer, J. E.; Dai, H.; Thess, A.; Lee, R.; Hanjani, N. M.; Dehaas, D. L.; Smalley, R. E. *Phys. Rev. B* **1997**, *55*, R4921.
(22) Lau, K. T.; Hui, D. *Composites, Part B* **2002**, *33*, 263.
(23) Lourie, O.; Wagner, H. D. *Appl. Phys. Lett.* **1998**, *73*, 3527.
(24) Shaffer, M. S.; Windle, A. H. *Adv. Mater.* **1999**, *11*, 937.
(25) Jia, Z.; Wang, Z.; Xu, C.; Liang, J.; Wei, B.; Wu, D.; Zhu, S. *Mater. Sci. Eng., A* **1999**, *271*, 395.
(26) Ajayan, P. J.; Schadler, L. S.; Giannaris, C.; Rubio, A. *Adv. Mater.* **2000**, *12*, 750.
(27) Gong, X.; Liu, J.; Baskaran, S.; Voise, S.; Young, J. S. *Chem. Mater.* **2000**, *12*, 1049.
(28) Jin, Z.; Pramoda, K. P.; Xu, G.; Goh, S. H. *Chem. Phys. Lett.* **2001**, *337*, 43.
(29) Pötschke, P.; Fornes, T. D.; Paul, D. R. *Polymer* **2002**, *43*, 3247.
(30) Coleman, J. N.; Curran, S.; Dalton, A. B.; Davey, A. P.; MacCarthy, B.; Blau, W.; Barklie, R. C. *Phys. Rev. B* **1998**, *58*, R7492.
(31) Curran, S. A.; Ajayan, P. M.; Blau, W. J.; Caroll, D. L.; Coleman, J. N.; Dalton, A. B.; Davey, A. P.; Drury, A.; McCarthy, B.; Maier, S.; Strevens, A. *Adv. Mater.* **1998**, *10*, 1091.
(32) Sandler, J.; Shaffer, M. S. P.; Prasse, T.; Bauhofer, W.; Schulte, K.; Windle, A. H. *Polymer* **1999**, *40*, 5967.
(33) Fan, J.; Wan, M.; Zhu, D.; Chang, B.; Pan, Z.; Xie, S. *J. Appl. Polym. Sci.* **1999**, *74*, 2605.
(34) Benoit, J.-M.; Corraze, B.; Lefrant, S.; Blau, W. J.; Bernier, P.; Chauvet, O. *Synth. Met.* **2001**, *121*, 1215.
(35) Kymakis, E.; Alexandou, I.; Amaratunga, G. A. J. *Synth. Met.* **2002**, *127*, 59.
(36) Kilbride, B. E.; Coleman, J. N.; Fraysse, J.; Fournet, P.; Cadek, M.; Drury, A.; Hutzler, S.; Roth, S.; Blau, W. J. *J. Appl. Phys.* **2002**, *92*, 4024.
(37) Stéphan, C.; Thien Phap, N.; Lahr, B.; Blau, W.; Lefrant, S.; Chauvet, O. *J. Mater. Res.* **2002**, *17*, 396.
(38) Yosida, Y.; Oguro, I. J. *J. Appl. Phys.* **1999**, *86*, 999.
(39) Hilt, O.; Brom, H. B.; Ahlskog, M. *Phys. Rev. B* **2000**, *61*, R5129.
(40) Stauffer, G. In *Introduction to Percolation Theory*; Taylor & Francis: London, 1985.
(41) Bacsa, R. R.; Laurent, C.; Peigney, A.; Bacsa, W. S.; Vaugien, T.; Rousset, A. *Chem. Phys. Lett.* **2000**, *323*, 566.
(42) Flahaut, E.; Peigney, A.; Laurent, C.; Rousset, A. *J. Mater. Chem.* **2000**, *10*, 249.
(43) Jonscher, A. K. *Nature (London)* **1977**, *267*, 673.
(44) Dyre, J. C.; Schroder, T. B. *Rev. Mod. Phys.* **2000**, *72*, 873.
(45) Reghu, M.; Yoon, C. O.; Yang, C. Y.; Moses, D.; Smith, P.; Heeger, A. J. *Phys. Rev. B* **1994**, *50*, 13931.
(46) Fraysse, J.; Planes, J. *Phys. Status Solidi B* **2000**, *218*, 273.
(47) Gubbels, F.; Jerome, J.; Teyssie, P.; Vanlathem, E.; Deltour, R.; Calderone, A.; Parente, V.; Bredas, J. L. *Macromolecules* **1994**, *27*, 1972.
(48) Balberg, I.; Anderson, C. H.; Alexander, S.; Wagner, N. *Phys. Rev. B* **1984**, *30*, 3933.
(49) Benoit, J.-M. Ph.D. Thesis, Nantes University, France, 2001.
(50) Krstic, V.; Muster, J.; Duesberg, G. S.; Philipp, G.; Burghard, M.; Roth, S. *Synth. Met.* **2000**, *110*, 245.
(51) Watts, P. C. P.; Hsu, W. K.; Chen, G. Z.; Fray, D. J.; Kroto, H. W.; Walton, D. R. M. *J. Mater. Chem.* **2001**, *11*, 2482.

(52) Kim, G. T.; Jhang, S. H.; Park, J. G.; Park, Y. W.; Roth, S. *Synth. Met.* **2001**, *117*, 123.
(53) Barrau, S.; Demont, P. Private communication, 2002.
(54) Sichel, E. K.; Gittelman, J. I.; Sheng, P. *Phys. Rev. B* **1978**, *18*, 5712.
(55) Sheng, P. *Phys. Rev. B* **1980**, *21*, 2180.
(56) Connor, M. T.; Roy, S.; Ezquerra, T. A.; Balta Calleja, J. *Phys. Rev. B* **1998**, *57*, 2286.
(57) Cramer, C.; Buscher, M. *Solid State Ionics* **1998**, *105*, 109.
(58) Roling, B. *Solid State Ionics* **1998**, *105*, 185.
(59) Kulkarni, A. R.; Lukenheimer, P.; Loidl, A. *Solid State Ionics* **1998**, *112*, 69.
(60) Pike, G. E. *Phys. Rev. B* **1972**, *6*, 1572.
(61) Elliot, S. R. *Adv. Phys.* **1987**, *36*, 185.

MA021263B